Fluoxetine targets early progenitor cells in the adult brain

Juan M. Encinas, Anne Vaahtokari, and Grigori Enikolopov*

Cold Spring Harbor Laboratory, Cold Spring Harbor, NY 11724

Communicated by James D. Watson, Cold Spring Harbor Laboratory, Cold Spring Harbor, NY, March 15, 2006 (received for review January 19, 2006)

Chronic treatment with antidepressants increases neurogenesis in the adult hippocampus. This increase in the production of new neurons may be required for the behavioral effects of antidepressants. However, it is not known which class of cells within the neuronal differentiation cascade is targeted by the drugs. We have generated a reporter mouse line, which allows identification and classification of early neuronal progenitors. It also allows accurate quantitation of changes induced by neurogenic agents in these distinct subclasses of neuronal precursors. We use this line to demonstrate that the selective serotonin reuptake inhibitor antidepressant fluoxetine does not affect division of stem-like cells in the dentate gyrus but increases symmetric divisions of an early progenitor cell class. We further demonstrate that these cells are the sole class of neuronal progenitors targeted by fluoxetine in the adult brain and suggest that the fluoxetine-induced increase in new neurons arises as a result of the expansion of this cell class. This finding defines a cellular target for antidepressant drug therapies.

hippocampus | neural stem cells | neurogenesis | dentate gyrus | antidepressants

Antidepressant drugs of the selective serotonin reuptake inhibitor (SSRI) class (e.g., fluoxetine) are commonly used to treat a wide spectrum of mood disorders in adults (1); they also are increasingly prescribed to children and adolescents (2, 3). However, the cellular basis for the action of SSRIs is not clear. In addition to its effects on neurotransmission, SSRI fluoxetine increases generation of new neurons in the dentate gyrus (DG) of the adult brain (4–9). Importantly, recent findings suggest that this increase may be a causative factor in the behavioral effects of this class of antidepressants (7). These discoveries may provide a novel framework for understanding depression and designing new therapeutic drugs. However, the step within the neuronal differentiation cascade targeted by SSRIs remains unknown. Particular targets (e.g., stem cells vs. early progenitors vs. advanced neuroblasts) may imply different molecular mechanisms of controlling cell division and survival, different circuits affected by the drugs, and different insights on the behavioral action of the drugs.

One of the problems in defining SSRI targets within the neuronal proliferation-differentiation cascade is the imprecision in quantifying the changes in each class of neural precursor cells in the brain. Accurate enumeration of changes in distinct subpopulations of neuronal precursors by immunocytochemistry is problematic: High cell density, complex cell morphology, and uncertainties in defining distinct boundaries between subclasses of cells reduces the precision of evaluating changes in particular subclasses of neuronal precursors (e.g., in contrast to BrdU or thymidine labeling of cell nuclei, where great precision can be achieved); this problem is particularly acute in the young brain, where the number of neural stem and progenitor cells is particularly high. Likewise, functional *in vitro* assays for identifying neural stem and progenitor cells (e.g., formation of neurospheres) are unable to provide confident measures of changes on a scale commensurate with the action of antidepressants [or many other reported inducers of neurogenesis (10, 11) that, in many cases, induce a 30–40% increase in the number of newly generated cells); furthermore, such assays presently cannot be performed for small subregions of neurogenic areas.

To circumvent these problems, we have generated a reporter mouse line that allows a quantitative assessment of changes in the stem/progenitor cell compartment of the adult brain. We used this line to divide the neuronal differentiation cascade into several easily discernable steps. We then used this reporter line to show that the SSRI antidepressant fluoxetine affects a specific step of this cascade in the adult brain, increasing symmetric divisions of a particular early neural progenitor class in the DG.

Results

Defined Steps in the Neurogenesis Cascade in the DG. Expression of nestin marks neural stem and progenitor cells; the regulatory elements of the nestin gene direct reporter gene expression to the neuroepithelium of the embryo and to stem and progenitor cells of the adult brain (12–16). We used these elements to generate a transgenic mouse line in which the reporter, a cyan fluorescent protein, is fused to a nuclear localization signal (CFPnuc). The CFPnuc reporter is expressed in these nestin-CFPnuc animals in the developing nervous system and in the neurogenic areas of the adult brain [the DG, subventricular zone (SVZ), rostral migratory stream, and olfactory bulb]. Importantly, the distribution of the stem/progenitor cells in the neurogenic areas of these mice can be visualized as a dotted pattern corresponding to the nuclei of these cells. This nuclear representation of stem/progenitor cells greatly reduces the complexity of their distribution pattern and permits their unambiguous enumeration (thus capturing the power of BrdU- or thymidine-based enumeration of nuclei). Fig. 1 *A–F* compares the structures of the SVZ and DG as revealed by immunochemistry for nestin and by expression of nestin-CFPnuc or nestin-GFP (13). Whereas we were unable to generate accurate counts of nestin- or nestin-GFP-positive cells, we were able to unambiguously enumerate (by using confocal stereology) all of the labeled nuclei in the SVZ and DG of the nestin-CFPnuc mice.

We have used this nestin-CFPnuc reporter line to define discrete steps in the neuronal differentiation cascade in the DG (leading from stem/progenitor cells to differentiated granule neurons), based on the morphology of the cells, the marker proteins that they express, and their mitotic activity (measured by BrdU incorporation). We identify six classes of cells in the neuronal lineage in the DG of nestin-CFPnuc mice (Figs. 1 and 2).

The first class is represented by glial fibrillary acidic protein (GFAP)-positive nestin-CFPnuc cells. The triangular soma and the nuclei of these cells reside in the subgranular zone (SGZ); they extend a single- or double-apical process radially across the granule

Conflict of interest statement: No conflicts declared.

Freely available online through the PNAS open access option.

Abbreviations: ANP, amplifying neuroprogenitor; DG, dentate gyrus; Dcx, doublecortin; GCL, granule cell layer; GFAP, glial fibrillary acidic protein; IN, immature neuron; NB 1, type 1 neuroblasts; NB 2, type 2 neuroblasts; NeuN, neuronal nuclei; Prox-1, homeobox prospero-like protein; PSA-NCAM, polysialic-acid neural cell adhesion molecule; QNP, quiescent neuroprogenitor; SGZ, subgranular zone; SSRI, selective serotonin reuptake inhibitor; SVZ, subventricular zone.

*To whom correspondence should be addressed. E-mail: enik@cshl.edu.

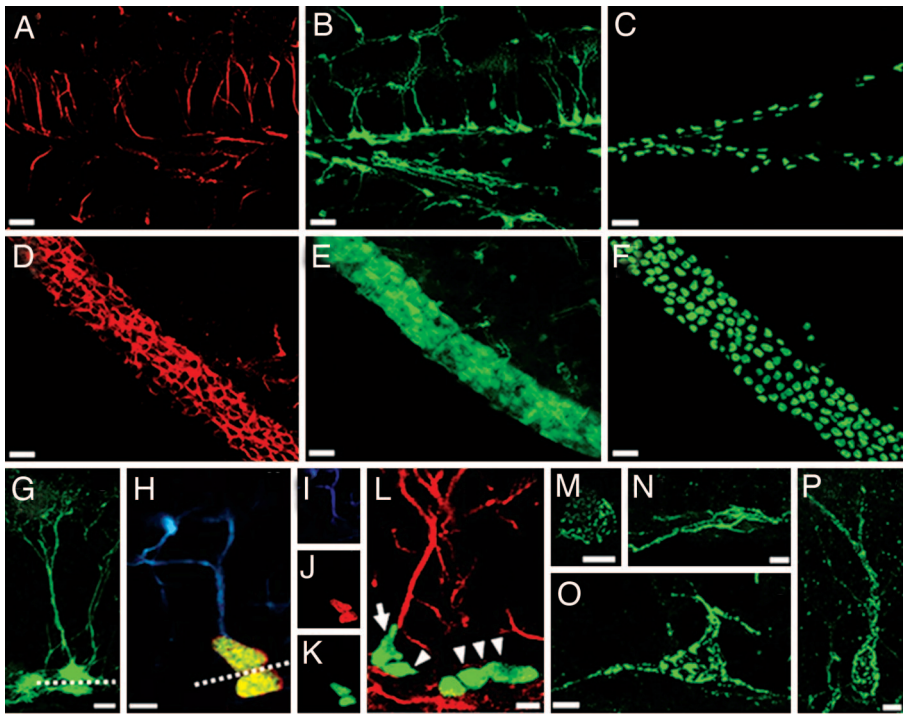

Fig. 1. Defining neuronal differentiation cascade in the DG. (*A*) Expression of endogenous nestin, detected by using a monoclonal antibody, in the DG of nestin-GFP transgenic mice; the pattern was the same in WT animals. (*B*) Expression of GFP in the DG of nestin-GFP transgenic mice; note that endogenous nestin in *A* is seen mostly in the processes, whereas GFP is present in the processes, the cytoplasm, and the nucleus. Tight packing of cells in the SGZ prevents accurate enumeration of nestin-GFP expressing cells. (*C*) Expression of CFPnuc, detected by using a polyclonal antibody in the SGZ of nestin-CFPnuc mice; transgene-expressing cells now are represented by their nuclei, thus making accurate cell counts even in densely packed areas possible. (*D–F*) Expression of nestin (*D*) and GFP (*E*) in the SVZ of nestin-GFP mice and CFPnuc (*F*) in the SVZ of nestin-CFPnuc mice. Note that densely packed SVZ cells, which cannot be accurately counted in *D* or *E*, can be quantified easily in *F*. (*G*) GFP-expressing neural progenitor cells in the DG of the nestin-GFP mice. The soma of both QNP and ANP cells is seen in the SGZ; QNP cells carry vertical processes, which cross the granule cells layer and end as elaborated arbors in the molecular layer (processes also can be visualized by an antibody to GFAP). ANP cells lack the processes; during and immediately after division, they can be seen in close contact with QNP (note a QNP and an ANP cell above and beneath the dashed line). (*H–K*) Asymmetric division of stem-like QNP cells in the DG generates ANP cells. (*H*) After BrdU labeling, cells with GFAP-labeled processes can be seen dividing (note the horizontal plane of division, dashed line) and generating daughter cells that are deposited below, do not carry processes or arbors, and do not stain for GFAP. (*I–K*) Staining for GFAP (blue; *I*), BrdU (red; *J*), and CFPnuc (green; *K*). (*L*) A QNP cell (arrow) generates an ANP cell (arrowhead) through an asymmetric division, with the plane of division parallel to the SGZ. Nearby is a cluster of ANP cells (arrowheads) generated through symmetric divisions in the plane perpendicular to the SGZ. GFAP is red, and CFPnuc is green. (*M* and *N*) ANPs differentiate into NB1 cells, which start to express markers of young neurons. NB1 cells still are located in the SGZ, cease to express nestin or nestin-CFPnuc, and start to express PSA-NCAM (green), Dcx, and Prox-1. A small subclass of these cells (*M*) resembles the ANP cells morphologically and is the last cell population to incorporate BrdU. The majority of the NB1 cells (*N*) extends horizontal processes and does not incorporate BrdU. (*O*) NB1 cells evolve morphologically and are converted into NB2 cells. NB2 cells are largely confined to the SGZ and extend most of their processes horizontally; however, one process grows vertically or obliquely and extends into the GCL. These cells express PSA-NCAM (green), Dcx, Prox-1, and NeuN. (*P*) NB2 cells progress into IN. The morphology of these cells resembles that of mature granule neurons. They extend a single vertical apical process and have their soma in the granule cell layer. They express NeuN and Prox-1 but still express PSA-NCAM (green) and Dcx. (Scale bars: *A–F*, 20 μm; *G*, *H*, *L–P*, 5 μm.)

cell layer (GCL), terminating with elaborated arbors of very fine leaf-like processes in the molecular layer (Fig. 1 *G–K*; see also ref. 13). This characteristic apical process is easily visualized with antibodies to GFAP, nestin, vimentin, and brain fatty acid-binding protein. Cells of this class have been described in detail (13, 17–21), and they correspond to the most primitive, stem-like population in the DG; note, however, that not all of the criteria of stem cells, e.g., ability to self-renew, have been demonstrated for these cells (22–24). Only a small fraction of these cells ($<2\%$) can be labeled by BrdU after a short (2-h) pulse, indicating their low rate of division and consistency with the quiescent state of these cells (18, 20); we therefore designate these cells as quiescent neural progenitors (QNP). We have not been able to detect instances of symmetric division of such cells (i.e., generating two similar cells or keeping the plane of division perpendicular to the SGZ); however, these cells can be seen undergoing asymmetric divisions (below).

The second class is represented by small (somatic diameter $\approx$10 μm) round or oval cells located in the SGZ (Fig. 1 *H–K*). Similar to QNPs, these cells express nestin-CFPnuc, brain fatty acid-binding protein, and Sox2, but they do not stain for GFAP or vimentin and stain very weakly for nestin (which may indicate that CFPnuc protein persists in these cells longer than nestin, or that nestin is unequally distributed during cell division); they also do not stain for doublecortin (Dcx), polysialic-acid neural cell adhesion molecule (PSA-NCAM), or for markers of differentiated neurons [homeobox prospero-like protein (Prox-1), βIII-tubulin, neuronal nuclei (NeuN), or calbindin]. These cells are labeled with BrdU at high frequency (20–25% 2 h after a single injection of BrdU), indicating that most of them are involved in mitotic activity; we designate these cells as amplifying neural progenitors (ANP). They are often seen in clusters extending along the SGZ (Fig. 1*L*); when the plane of division of cells in these clusters is visible, it is most often perpendicular to the SGZ, such that the daughter cells remain in the SGZ (Fig. 1*L*). Importantly, a fraction of these cells are seen separating from QNPs after mitosis; in each case, the division plane is parallel or slightly oblique to the SGZ such that the daughter cell is deposited beneath the QNP cell (Fig. 1 *H–K*) (the plane of division may explain why these cells do not inherit GFAP or nestin, which are predominantly localized to the apically positioned processes of the QNPs but not to their soma). Together, our results suggest that QNP cells, by undergoing asymmetric divisions, give rise to ANP cells, which then propagate in the SGZ through a series of symmetric divisions.

The next class of precursor cells, still located in the SGZ, ceases to express nestin, Sox2, brain fatty acid-binding protein, or CFPnuc and starts to express Dcx and PSA-NCAM (Fig. 1 *M* and *N*). A small subclass ($\approx$1% of cells in this class) morphologically resembles ANPs, carries short (1–5 μm) horizontal processes (Fig. 1*M*), and is the final population in the differentiation cascade that is labeled by BrdU (19). Most of the cells in this class are represented by larger (10–15 μm somatic diameter) cells that extend longer (10–30 μm) horizontal processes in the plane of the SGZ and do not incorporate BrdU (Fig. 1*N*). These cells stain for Dcx, PSA-NCAM, Prox-1, and βIII-tubulin but do not express NeuN. Thus, the bulk of this class is represented by postmitotic neuronal precursors; we designate them as type 1 neuroblasts (NB1).

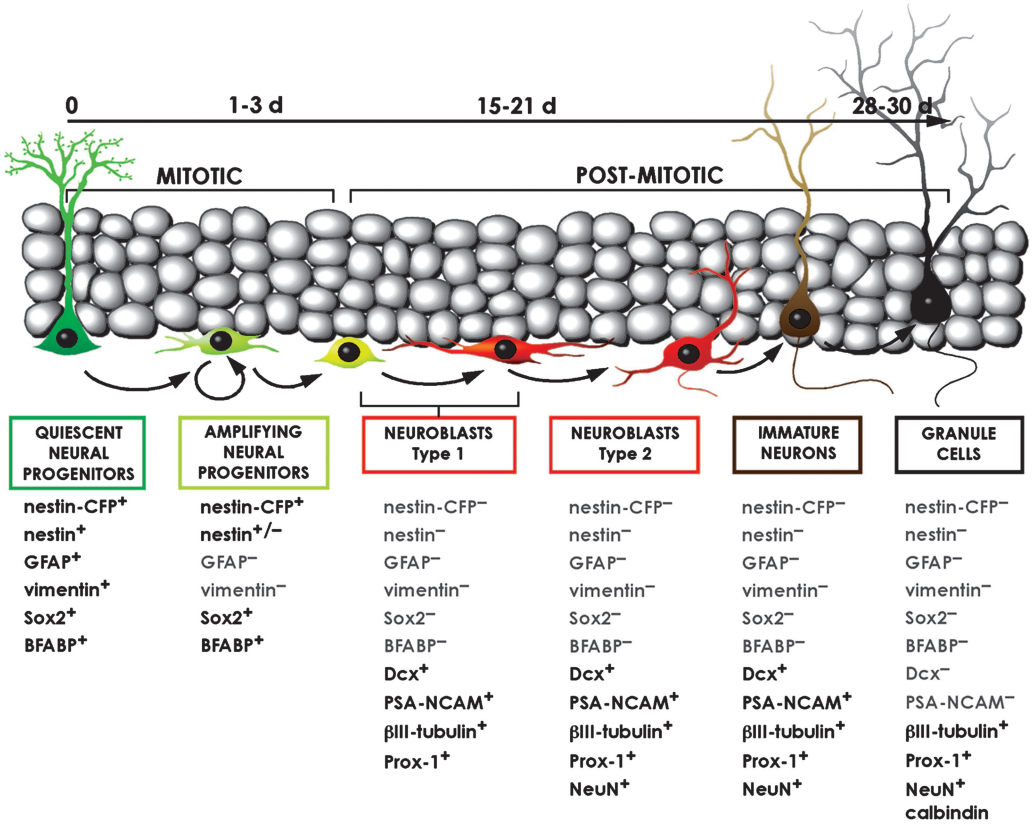

Fig. 2. A schematic summary of the neuronal differentiation cascade in the DG. QNPs generate, through asymmetric divisions, the ANPs that, after several rounds of symmetric divisions, exit the cell cycle within 1–3 days and become postmitotic NB1 cells. Within next 15–21 days, NB1 cells mature into NB2 and then into IN with apical processes and basal axons and the soma located in the GCL. After an additional 10–15 days, INs acquire the characteristics of mature granule neurons, develop extensive branching, and send long axonal processes, forming the mossy fiber.

Cells of the next class, type 2 neuroblasts (NB2), are larger than NB1 cells (somatic diameter ≈15 μm) and remain confined to the SGZ. They extend longer (20–40 μm) processes horizontally and obliquely to the plane of the SGZ (Fig. 1*O*). They do not express QNP or ANP markers (nestin, GFAP, vimentin, Sox2, brain fatty acid-binding protein, or CFPnuc), and express Dcx, PSA-NCAM, Prox-1, βIII-tubulin, and NeuN.

The next class of cells corresponds to immature neurons (IN). They are larger than the cells of the previous classes (somatic diameter 15–20 μm), and their morphology resembles that of mature granule cells of the DG (Fig. 1*P*). Their soma is round or oval and can be found both in the SGZ and, mainly, in the GCL. These cells carry a single apical process that branches in its distal part located in the molecular layer. They express Dcx, PSA-NCAM, Prox-1, βIII-tubulin, and NeuN.

The next class represents differentiated granule neurons, with developed apical dendrites and axons forming the mossy fiber. They cease to express PSA-NCAM and Dcx but express Prox-1, βIII-tubulin, NeuN, and markers of mature granule neurons (e.g., calbindin; ref. 25).

The differentiation cascade in the DG of nestin-CFPnuc mice thus can be divided into discrete steps based on the expression of markers, morphology, and mitotic activity (Fig. 2).

Fluoxetine Increases Symmetric Divisions of Early Progenitors in the DG. Chronic treatment with fluoxetine increases the number of new neurons in the DG (4–9). Note, however, that these observations do not reveal the identity of cells targeted by the drug; this increase can potentially reflect changes in stem/progenitor cells, advanced neuroblasts, immature neurons, or in some combination of these classes. We used our nestin-CFPnuc reporter line to investigate changes induced by fluoxetine in each of the classes we identified in the DG. We treated the animals with fluoxetine for 15 days, labeled dividing cells with BrdU, and monitored selected cell populations in the DG after 24 h by using confocal stereology (Fig. 3). The number of BrdU-labeled cells in the DG was increased by 40.9% (538 ± 51 vs. 758 ± 58; $P = 0.013$) after fluoxetine administration, in line with previous reports on the effects of chronic treatment with the drug (refs. 4 and 7; Fig. 3 *A–C*). We also found that after treatment, the number of CFPnuc-positive cells (i.e., QNPs and ANPs together) increased by 24.7% (8,356 ± 622 vs. 10,422 ± 646; $P = 0.037$; Fig. 3 *D–F*). When these cells were divided into QNP and ANP classes based on expression of GFAP, the QNP class showed no change (4,516 ± 582 vs. 4,675 ± 518; Fig. 3*G*), whereas the number of ANP cells increased by 49.6% (3,840 ± 431 vs. 5,745 ± 506; $P = 0.012$; Fig. 3*H*). No change was detected in the volume of the GCL, including the SGZ, between the control and experimental animals (0.468 ± 0.039 vs. 0.483 ± 0.052 mm^3).

The number of PSA-NCAM-positive cells (which include NB1, NB2, and IN cells, Fig. 4 *A* and *B*) was increased by 26.5 ± 7.2% (8,936 ± 577 vs. 11,298 ± 719; $P = 0.022$) (identical changes were seen for Dcx-positive cells; note that Dcx and PSA-NCAM colocalized in both control and fluoxetine-treated animals; data not shown). When these cells were subdivided further by using the criteria described above, the number of NB1 cells was increased by 42.1% (4,918 ± 418 vs. 6,988 ± 538; $P = 0.089$; Fig. 4*C*), and the number of NB2 and IN cells remained unchanged (3,110 ± 209 vs. 3,452 ± 413 and 908 ± 11 vs. 858 ± 88, respectively) (Fig. 4 *D* and *E*), compatible with the notion that the wave of increased proliferation and differentiation has not reached those cell classes.

Thus, the earliest class affected by fluoxetine is the ANP cells which are progeny of stem-like QNP cells. Importantly, the QNPs themselves do not increase in number, consistent with the lack of symmetrical divisions in this class. The increase in ANPs can be due to either (*i*) an increased rate of asymmetric divisions of QNPs (i.e., QNPs may be dividing more often under the influence of fluoxetine but only give rise to daughter ANP cells while keeping their own number constant) or (*ii*) increased symmetric division of ANP cells (i.e., the same number of ANPs may be born from QNPs, but they then divide more frequently). To distinguish between these possi-

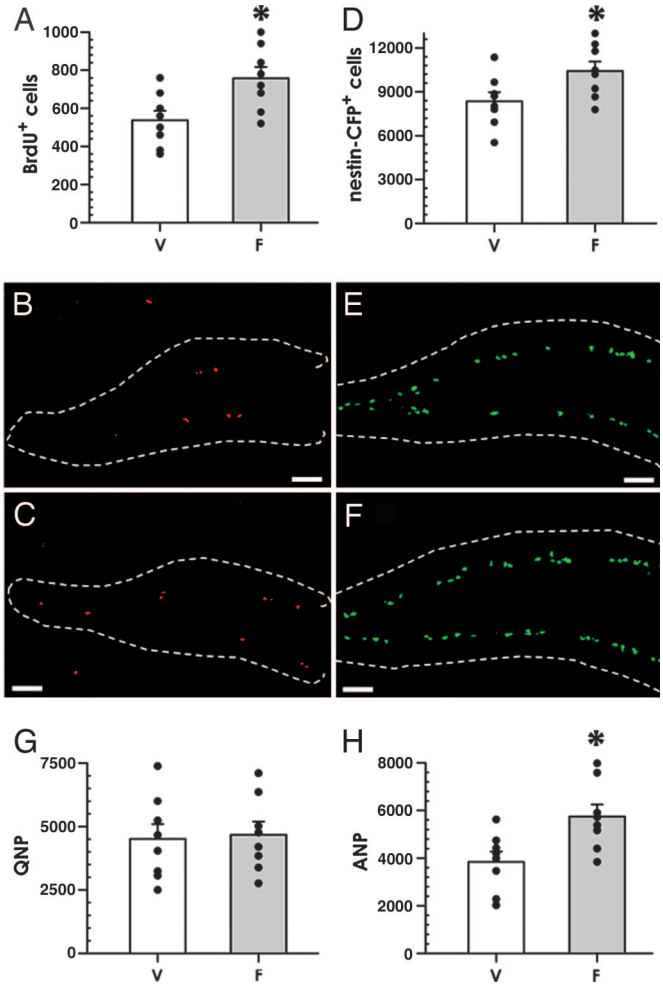

Fig. 3. Fluoxetine increases cell proliferation in the adult DG. Chronic (15 days) fluoxetine treatment of adult (7 months) mice, analyzed 1 day after BrdU administration. Fluoxetine increases the number of BrdU-positive cells (*A*). (*B* and *C*) Representative photomicrographs of DG sections from animals treated with vehicle (*B*) and fluoxetine (*C*); dashed lines in *B*, *C*, *E*, and *F* outlines the external limits of the DG. Exposure to fluoxetine also increases the number of nestin-CFPnuc cells in the SGZ (*D*, histogram; *E*, section of the DG of a control animal; *F*, section of the DG of a fluoxetine-treated animal). Within total nestin-CFPnuc cells, the number of ANPs (*H*), but not QNPs (*G*), increases in response to fluoxetine. (Scale bars: 50 μm.) In all histograms, white bars correspond to the vehicle injections (V), and gray bars to the fluoxetine injections (F). Error bars show SEM. The results for individual animals ($n = 8$ per group in this figure) are shown as black dots. *, $P < 0.05$.

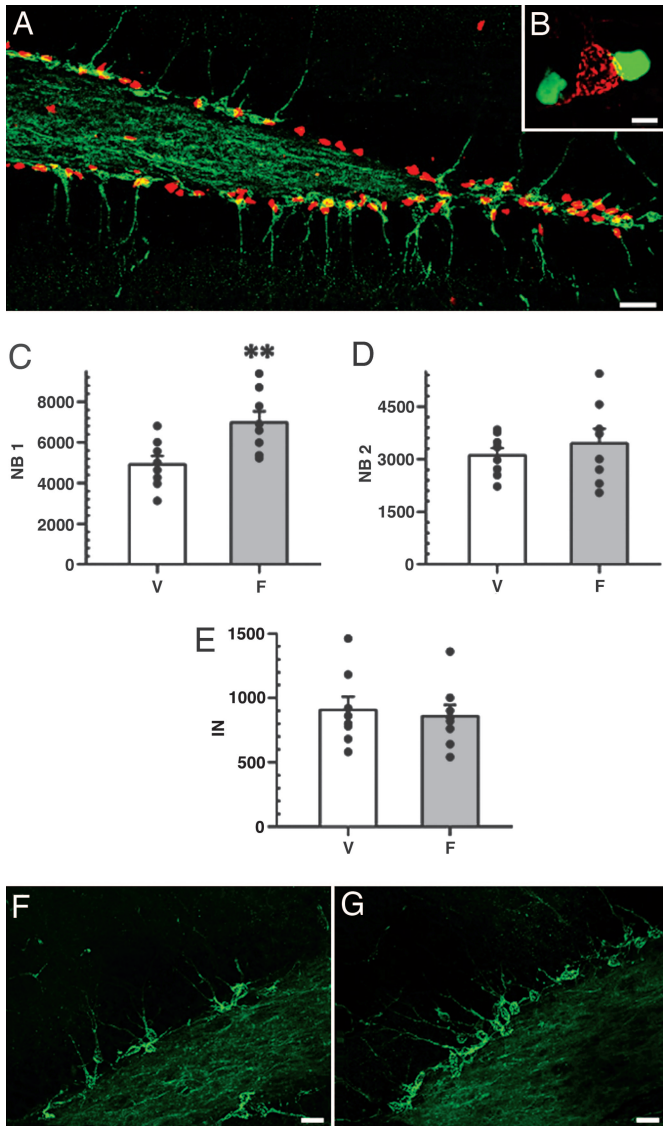

Fig. 4. Fluoxetine increases NB1 cells in the adult DG. (*A* and *B*) Immunostaining for PSA-NCAM (green), and nestin-CFPnuc (red). Two cell types are distributed throughout the SGZ, often in close apposition to each other; however, they do not overlap, as illustrated in *B* (PSA-NCAM cell is red, and nestin-CFPnuc nuclei are green; note that colors are switched at low magnification for better visualization). (*C–G*) Postmitotic precursors in the fluoxetine-treated DG of adult mice, analyzed 1 day after BrdU labeling. Fluoxetine increases the number of NB1 (*C*) but not of more advanced NB2 (*D*) or IN (*E*) cells. V, vehicle; F, fluoxetine. $n = 8$ per group. **, $P < 0.01$. *F* and *G* are representative photomicrographs of DG from control (injected with vehicle) (*F*) and fluoxetine-treated (*G*) animals. (Scale bars: *A*, 20 μm; *B*, 5 μm; *F* and *G*, 10 μm.)

bilities, we counted the number of BrdU-labeled QNPs and ANPs. We used triple labeling (CFPnuc, BrdU, and GFAP) to discriminate between QNPs and ANPs and to quantify their mitotic activity (Fig. 5). The number of BrdU-labeled QNPs was not affected by fluoxetine treatment (83 ± 22 vs. 90 ± 16; $P = 0.8$; Fig. 5*A*), whereas the number of BrdU-labeled ANPs was increased 46.4% (280 ± 36 vs. 410 ± 33; $P = 0.023$; Fig. 5*B*); the fraction of dividing cells among QNPs (Fig. 5*C*) and ANPs (Fig. 5*D*) did not change. These results indicate that the rate of QNP cell division is unchanged and that fluoxetine increases symmetric divisions of ANP cells. When considered together with the data on other cell classes, these results suggest that ANPs are the only class of precursor cells in the DG that directly respond to fluoxetine.

We also analyzed the changes in the SVZ, another major neurogenic region (Fig. 7*A*, which is published as supporting information on the PNAS web site). We did not observe changes in the number of BrdU-labeled cells ($10{,}058 \pm 766$ vs. $9{,}550 \pm 769$; Fig. 7 *B*, *D*, and *E*), in agreement with the previous observations in rats (4). Furthermore, we did not find any significant changes either in the number of nestin-CFPnuc cells, (454 ± 52 vs. $473 \pm 55 \times 10^3$; Fig. 7 *C–E*), or in their density (648 ± 55 vs. $687 \pm 64 \times 10^3$ mm^3), or in the volume (0.648 ± 0.058 vs. 0.603 ± 0.051 mm^3) of the SVZ. Together, our data indicate that the fluoxetine-induced increase in the number of early progenitor cells is specific for the DG and does not affect the SVZ.

To investigate whether the fluoxetine-induced increase in progenitor cells is manifested later as an increase in the number of new neurons in the DG and whether the increase is maintained after the

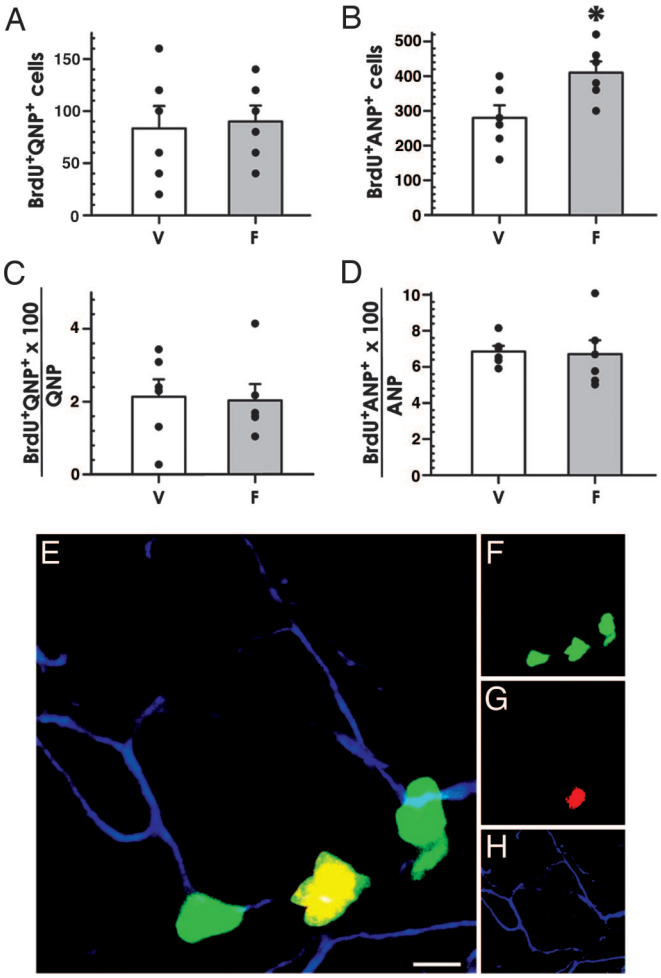

Fig. 5. Fluoxetine increases proliferation of ANP cells in the DG. (*A–D*) Treatment with fluoxetine does not change the number of dividing (BrdU-labeled) QNPs (*A*) but increases division of ANPs (*B*). The fraction of BrdU-labeled QNP or ANP cells among total QNP or ANP cells, respectively, remains the same (*C* and *D*). V, vehicle; F, fluoxetine. $n = 6$ per group. *, $P < 0.05$. (*E–H*) A cluster of BrdU-positive ANP cells between two QNPs in the DG of a fluoxetine-treated animal. QNP cells are identified by the presence of GFAP-positive processes. CFPnuc is shown in green (*F*), BrdU in red (*G*), and GFAP in blue (*H*). (Scale bar: 5 μm.)

cessation of treatment with fluoxetine, we performed the fluoxetine treatment and BrdU labeling as described above but killed the animals 30 days (instead of 1 day) later. In this setting, the number of BrdU-labeled cells was 46.2% higher in the fluoxetine-treated group (234 ± 28 vs. 342 ± 24; $P = 0.037$; Fig. 6*A*). The number of BrdU-labeled NeuN-positive neurons also was higher, by 46.3%, in the fluoxetine group (216 ± 26 vs. 316 ± 29; $P = 0.033$; Fig. 6 *B–E*). The fraction of $BrdU^+NeuN^+$ cells among total BrdU-positive cells did not change (92.7 ± 1.2 vs. 92.8 ± 1.6%; Fig. 6*C*); note that the high percentage of BrdU-labeled cells that also stain for NeuN indicates that with or without fluoxetine, the majority of surviving newborn cells in the DG become granule neurons. No change was detected in the volume of the GCL, including the SGZ, between the control and experimental animals (0.496 ± 0.041 vs. 0.512 ± 0.050 mm^3).

We also examined changes in the defined classes of precursor cells in mice killed 30 days after the end of the treatment with fluoxetine. Neither the total number of nestin-CFPnuc cells, nor the number of cells in QNP, ANP, NB1, NB2, or IN classes was changed (Fig. 6 *F–J*), suggesting that once the exposure to fluoxetine ends,

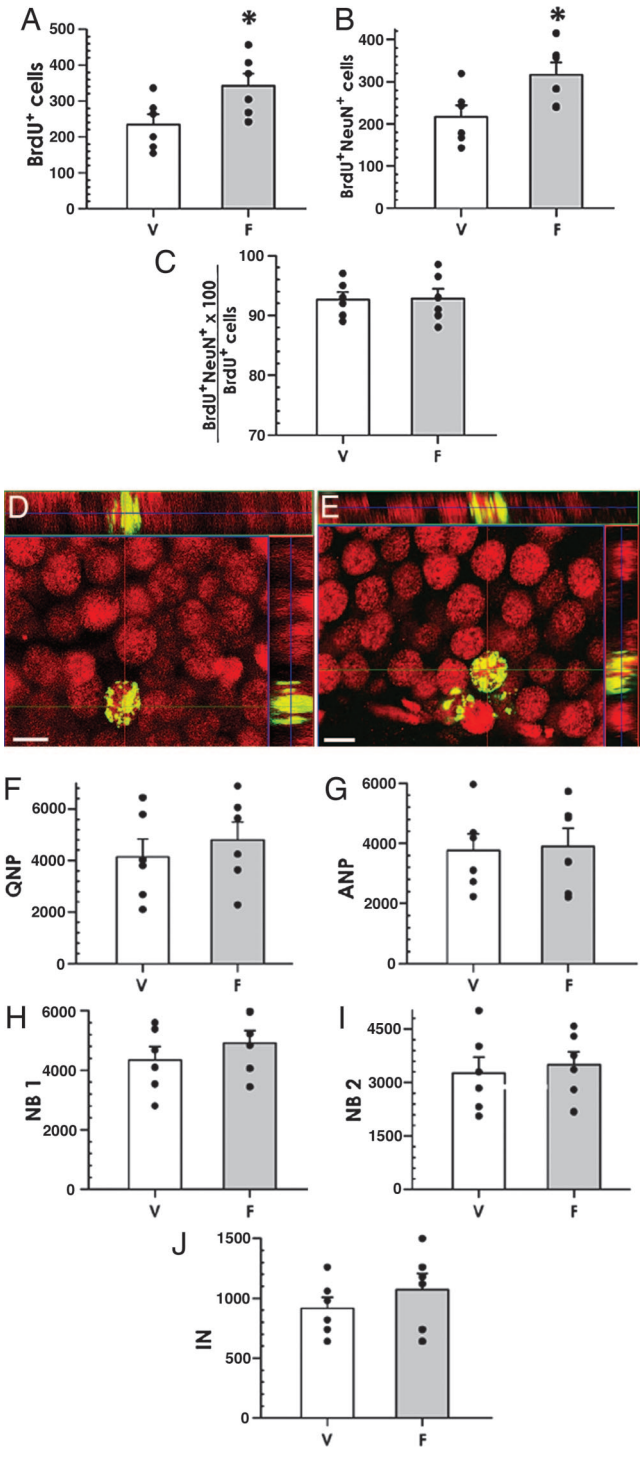

Fig. 6. Fluoxetine increases neurogenesis in the adult DG (30-day survival experiments). (*A–C*) Chronic fluoxetine treatment of adult mice, analyzed 30 days after BrdU administration. Fluoxetine increases the number of BrdU-positive cells in the DG (*A*), and the number of BrdU and NeuN double-positive cells (*B*); the fraction of such cells among total BrdU-positive cells remains the same (*C*). (*D* and *E*) Representative photomicrographs of DG from control (vehicle) (*D*) and fluoxetine-treated (*E*) animals show that new cells became neurons, shown by immunostaining for BrdU (green) and NeuN (red). The orthogonal projections are shown to confirm double labeling throughout the extent of positive cells. (Scale bars: 10 μm.) (*F–J*) Fluoxetine treatment does not increase the number of neuronal progenitors when analyzed 30 days after the treatment. The histograms show the data for the QNP (*F*), ANP (*G*), NB1 (*H*), NB2 (*I*), and IN (*J*) cells. Changes did not reach the level of significance in none of the categories. V, vehicle; F, fluoxetine. $n = 6$ per group. *, $P < 0.05$.

the rate of stem/progenitor cell division returns to its baseline rate. Together, these results suggest that the fluoxetine-induced increase in the number of ANP precursors in the DG later translates into an increase in the number of new neurons. They further suggest that the fate of the newborn cells remains unaltered, i.e., the vast majority of the surplus cells become granule neurons.

Discussion

We here present an approach for the quantitative dissection of the neurogenesis cascade and use this approach to show that fluoxetine targets a defined group of neuronal precursors in the DG. Our results link early progenitor cells to the action of SSRI antidepressants in the adult brain and suggest a strategy to investigate the changes induced by other antidepressant treatments.

Our approach circumvents several obstacles in assessing changes in cell number during neurogenesis, e.g., high cell density, which hinders precise counts, or uncertainty in attributing precursor cells to a particular class. It reduces the complex distribution pattern of precursor cells to a readily quantifiable punctate pattern of labeled nuclei. It allows unambiguous enumeration of cells in a particular precursor class and can be used to analyze changes induced by a wide range of stimuli in the developing or adult brain (8, 10, 11).

By using this approach, we identified six distinct classes of cells that comprise discrete steps in the differentiation cascade between neural stem cells and fully differentiated granule neurons; these classes can be distinguished easily by a combination of expressed markers and by morphology. They encompass and partially overlap with the categories of neuronal precursors defined by other approaches (13, 18–20, 25–28). For instance, QNP cells correspond most closely to cells described as subtype 2 astrocytes of the subgranular zone (17), GFAP-positive radially oriented cells of the DG (21), type 1 cells (18), GFP-bright cells (13), and rA cells (19); ANP cells include type 2a cells (18), NB1 cells include type 3 cells (18), and NB1, NB2, and IN classes overlap with D1, D2, and D3 cells (19). Our current scheme presents a detailed and complete description of the neuronal differentiation cascade in the DG. Further studies are needed to refine this classification and identify subclasses of precursor cells in the DG; for instance, our transcriptional profiling studies (unpublished data) suggest that ANPs can be further subdivided into smaller subpopulations, perhaps reflecting progressive division cycles.

Our results indicate that fluoxetine increases the rate of symmetric divisions of ANPs and that this increase is manifested later as an increase in the number of new neurons in the DG. Furthermore, they suggest that ANPs are the sole target of fluoxetine among the neurogenic cells in the adult nervous system, and that other drug-induced changes in neurogenesis and the eventual increase in new neurons arise as a consequence of this initial event. These results point to a defined step in the neuronal differentiation cascade affected by fluoxetine and provides a starting point to search for the circuits targeted by fluoxetine and for the molecular mechanisms of fluoxetine-induced signaling in the nervous system, for instance, understanding whether fluoxetine directly affects neural progenitors or acts indirectly through neighboring cells.

Materials and Methods

Transgenic Mice. Age-matched nestin-CFPnuc mice were used in this study. For details regarding the generation of this line, see *Supporting Materials and Methods*, which are published as supporting information on the PNAS web site.

Flouxetine Treatment. Seven-month old nestin-CFPnuc mice were injected with vehicle (distilled water) or with 10 mg/kg fluoxetine hydrochloride (Tocris Neuramin, Ellisville, MO) once per day for 15 days. On the last day, a single injection of BrdU (150 mg/kg) also was administered. Animals were killed either 24 h or 30 days after the end of the treatment and the BrdU injection.

Immunohistochemistry. Immunolabeling was performed by following standard protocols for tissue fixation and processing (see *Supporting Materials and Methods*).

Quantification. Quantitative analysis of cell populations was performed by means of design-based confocal-microscopy stereology. Details can be found in *Supporting Materials and Methods*.

We thank Sang Yong Kim and the Cold Spring Harbor Laboratory transgenic facility for generating the transgenic mice; Steven Hearn for the help with confocal microscopy; Barbara Mish for excellent assistance; Tatyana Michurina for help and discussions; and Tim Tully, Alex Koulakov, Amanda Sierra, Mirjana Maletic-Savatic, Natasha Peunova, and Julian Banerji for stimulating discussions and critical reading of the manuscript. J.M.E. is a Fellow of the Ministerio de Educación y Ciencia of Spain. G.E. is a Fellow of the Cody Center for Autism and Developmental Disabilities. Support was provided by the National Alliance for Research on Schizophrenia and Depression, the National Institute of Neurological Disorders and Stroke, The Hartman Foundation, The Ira Hazan Fund, The Seraph Foundation, and The Cody Center for Autism and Developmental Disabilities.

1. Wong, M. L. & Licinio, J. (2001) *Nat. Rev. Neurosci.* **2,** 343–351.
2. Whittington, C. J., Kendall, T., Fonagy, P., Cottrell, D., Cotgrove, A. & Boddington, E. (2004) *Lancet* **363,** 1341–1345.
3. Ryan, N. D. (2005) *Lancet* **366,** 933–940.
4. Malberg, J. E., Eisch, A. J., Nestler, E. J. & Duman, R. S. (2000) *J. Neurosci.* **20,** 9104–9110.
5. Jacobs, B. L., Praag, H. & Gage, F. H. (2000) *Mol. Psychiatry* **5,** 262–269.
6. Malberg, J. E. & Duman, R. S. (2003) *Neuropsychopharmacology* **28,** 1562–1571.
7. Santarelli, L., Saxe, M., Gross, C., Surget, A., Battaglia, F., Dulawa, S., Weisstaub, N., Lee, J., Duman, R., Arancio, O., *et al.* (2003) *Science* **301,** 805–809.
8. Lie, D. C., Song, H., Colamarino, S. A., Ming, G. L. & Gage, F. H. (2004) *Annu. Rev. Pharmacol. Toxicol.* **44,** 399–421.
9. Duman, R. S. (2004) *Biol. Psychiatry* **56,** 140–145.
10. Abrous, D. N., Koehl, M. & Le Moal, M. (2005) *Physiol. Rev.* **85,** 523–569.
11. Ming, G. L. & Song, H. (2005) *Annu. Rev. Neurosci.* **28,** 223–250.
12. Kawaguchi, A., Miyata, T., Sawamoto, K., Takashita, N., Murayama, A., Akamatsu, W., Ogawa, M., Okabe, M., Tano, Y., Goldman, S. A. & Okano, H. (2001) *Mol. Cell. Neurosci.* **17,** 259–273.
13. Mignone, J. L., Kukekov, V., Chiang, A. S., Steindler, D. & Enikolopov, G. (2004) *J. Comp. Neurol.* **469,** 311–324.
14. Roy, N. S., Wang, S., Jiang, L., Kang, J., Benraiss, A., Harrison-Restelli, C., Fraser, R. A., Couldwell, W. T., Kawaguchi, A., Okano, H., Nedergaard, M. & Goldman, S. A. (2000) *Nat. Med.* **6,** 271–277.
15. Yamaguchi, M., Saito, H., Suzuki, M. & Mori, K. (2000) *NeuroReport* **11,** 1991–1996.
16. Zimmerman, L., Parr, B., Lendahl, U., Cunningham, M., McKay, R., Gavin, B., Mann, J., Vassileva, G. & McMahon, A. (1994) *Neuron* **12,** 11–24.
17. Kosaka, T. & Hama, K. (1986) *J. Comp. Neurol.* **249,** 242–260.
18. Kronenberg, G., Reuter, K., Steiner, B., Brandt, M. D., Jessberger, S., Yamaguchi, M. & Kempermann, G. (2003) *J. Comp. Neurol.* **467,** 455–463.
19. Seri, B., Garcia-Verdugo, J. M., Collado-Morente, L., McEwen, B. S. & Alvarez-Buylla, A. (2004) *J Comp Neurol* **478,** 359–378.
20. Seri, B., Garcia-Verdugo, J. M., McEwen, B. S. & Alvarez-Buylla, A. (2001) *J. Neurosci.* **21,** 7153–7160.
21. Eckenhoff, M. M. F. & Rakic, P. P. (1984) *J. Comp. Neurol.* **223,** 1–21.
22. Bull, N. D. & Bartlett, P. F. (2005) *J. Neurosci.* **25,** 10815–10821.
23. Seaberg, R. M. & van der Kooy, D. (2002) *J. Neurosci.* **22,** 1784–1793.
24. Seaberg, R. M. & van der Kooy, D. (2003) *Trends Neurosci.* **26,** 125–131.
25. Brandt, M. D., Jessberger, S., Steiner, B., Kronenberg, G., Reuter, K., Bick-Sander, A., von der Behrens, W. & Kempermann, G. (2003) *Mol. Cell. Neurosci.* **24,** 603–613.
26. Filippov, V., Kronenberg, G., Pivneva, T., Reuter, K., Steiner, B., Wang, L. P., Yamaguchi, M., Kettenmann, H. & Kempermann, G. (2003) *Mol. Cell. Neurosci.* **23,** 373–382.
27. Fukuda, S., Kato, F., Tozuka, Y., Yamaguchi, M., Miyamoto, Y. & Hisatsune, T. (2003) *J. Neurosci.* **23,** 9357–9366.
28. Kempermann, G., Jessberger, S., Steiner, B. & Kronenberg, G. (2004) *Trends Neurosci.* **27,** 447–452.